MENOUFIA JOURNAL OF AGRICULTURAL ENGINEERING

https://mjae.journals.ekb.eg/

EFFECT OF WATER FLOW RATE AND AIR VELOCITY ON THE PERFORMANCE OF EVAPORATIVE COOLING SYSTEM FOR GREENHOUSE

Shokr, A. A.; Eissa, A. H.; El Saeidy, E. A. and Taha, A. T.

Agricultural and Biosystems Engineering Department, Faculty of Agriculture, Menoufia University, Shibin El-Kom, Egypt.

Received: Aug. 16, 2025 Accepted: Aug. 27, 2025

ABSTRACT: Climate change has become one of the most critical challenges affecting agricultural production worldwide. Environmental control inside greenhouses provides an effective strategy to mitigate the adverse impacts of such climatic variations. The primary objective of this study was to optimize the operational parameters of an evaporative cooling system, namely water flow rate and air velocity. To achieve this, experiments were conducted under three different water flow rates (2, 4, and 6 $L \cdot min^{-1} \cdot m^{-2}$) and three air velocities (1.0, 1.25, and 1.5 $m \cdot s^{-1}$), with and without shading nets. The effects of these parameters on greenhouse air temperature, relative humidity, cooling efficiency, and cooling capacity were evaluated. The findings revealed a clear correlation between indoor and outdoor air temperatures, where the indoor temperature followed the outdoor trend, increasing during the early morning, peaking at noon, and then declining as solar radiation decreased. Similarly, the relative humidity of the outdoor air increased during nighttime and decreased during daytime in response to the temperature rise. The results demonstrated that the maximum cooling efficiency (94.36%) was achieved at an air velocity of 1.25 $m \cdot s^{-1}$ and a water flow rate of 4 $L \cdot min^{-1} \cdot m^{-2}$ in the presence of shading nets. In contrast, the highest cooling capacity (91.96 kW) was obtained at an air velocity of 1.5 $m \cdot s^{-1}$ with the same water flow rate under shaded conditions. In general, the most efficient performance is achieved by operating the evaporative cooling system with shading nets at a water flow rate of 4 $L \cdot min^{-1} \cdot m^{-2}$ and an air velocity of 1.25 $m \cdot s^{-1}$. This combination not only maximizes cooling efficiency but also contributes to achieving a more stable greenhouse microclimate.

Keywords: Evaporative Cooling, Relative Humidity, Cooling Efficiency, Cooling Capacity.

INTRODUCTION

Greenhouses are enclosed environments that generate their own microclimate. This allows farmers to regulate inputs and outputs, including heating, cooling, temperature, humidity, CO_2 enrichment, and fertigation. The result is a favorable environment for plant growth and development. When compared to field-grown crops, greenhouses provide 5-10 times greater yields per unit area and have 5-10 times higher water usage efficiency. So, Closed greenhouses can also boost production rates, water saving, and sustainable management. (Graamans *et al.*, 2018).

By employing the proper cooling, ventilation, and shading techniques, greenhouses can maintain their climatic parameters during the summer months by keeping the internal air temperature and relative humidity within predetermined ranges. Despite this, cooling techniques have a significant impact on the distribution of greenhouse microclimate parameters, particularly on-air temperature and relative humidity. These two characteristics are thought to be the most important determinants of crop growth quality and uniformity. (Jin Ryu *et al.*, 2014).

Cooling is recognized as a critical requirement for greenhouse crops growing in tropical and subtropical nations to address the issue of high temperatures during the summer months. The creation of a proper cooling system that produces a favorable microclimate for crop growth is a complex challenge since the design is

* Corresponding author: ahmedshukr702@gmail.com

inextricably linked to local climatic circumstances. Cooling methods include natural and forced ventilation, shade screens and nets, and evaporative cooling systems. (Lee and Lee, 2013).

The evaporative cooling system is the most commonly used method for controlling greenhouse temperatures and has been the subject of numerous studies. The principle behind evaporative cooling is to use latent cooling provided by evaporated water to cool the air stream. This process is isenthalpic: that is, while it reduces the temperature of the air stream, the air stream's humidity increases. Evaporative cooling systems for covered crops are roughly classified into three types based on how water and air are fed and moved: fogging (misting), fan-pad evaporative cooling, and roof evaporative cooling. The descriptions of these systems are provided below. (Xu *et al.*, 2015).

When a study was conducted on the effect of air velocity on temperature reduction and cooling efficiency in fan pad evaporative cooling systems, it was suggested that the optimum air velocity passing through the pad should be greater than 0.5 ms^{-1} and less than 1.5 ms^{-1}. Dağtekin *et al.* (2011).

Water's high thermal capacity and high latent heat of evaporation make it an excellent cooling factor. Research on the water consumption of cellulose pads used for evaporative cooling in greenhouses revealed that, at incoming airflow velocities ranging from 1 to 1.5 m s^{-1}, the water consumption ranged from 1.8 to 2.6 L h^{-1} m^{-2} $^{o}c^{-1}$ (Franco *et al.*, 2010).

Shading is a potential strategy for controlling plant development characteristics while lowering agricultural production costs, such as the quantity of water required for irrigation and energy usage. Shading the greenhouse is an efficient way to provide a conducive environment for crop development while also increasing crop production and quality in hot and sunny places. As a result, crop output and quality improve, while energy and water usage is reduced. (Ahmed *et al.*, 2016).

The main goal of the study is to validate a pad fan evaporative cooling system by selecting the most effective parameters under the impact of evaporative cooling system variables such as air velocities and water flow rates, as well as employing a shade screen with these factors.

MATERIALS AND METHODS

The experimental work was carried out between August 2022 and August 2024 at the experimental farm of the Faculty of Agriculture, Menoufia University, Egypt, located at a latitude of 30°54′ N. The setup consisted of two modified Quonset-type greenhouses, each equipped with an evaporative cooling system and a shading net. Each greenhouse had a length of 6.0 m, a width of 3.0 m, and a total height of 3.9 m, with side walls of 2.0 m and an arch height of 1.9 m, giving a net floor area of 18 m^2. The supporting structure was fabricated from galvanized steel pipes with a diameter of 1 inch. A single polyethylene film of 200 µm thickness, treated against ultraviolet degradation, was used as the covering material. Both greenhouses were aligned along the north–south axis, which was identified as the most suitable orientation to enhance solar energy penetration, as presented in Fig. 1.

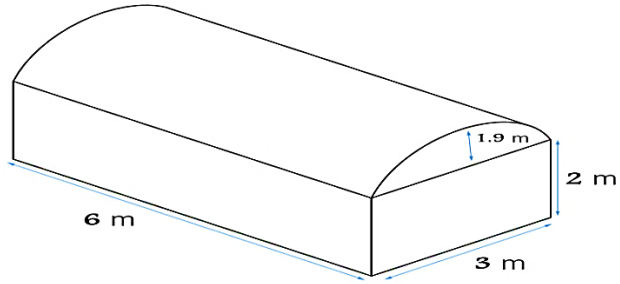

Fig. 1: Greenhouse dimensions.

Description of the fan pad Cooling System

The suggested cooling system is primarily composed of four main parts: a cellulose pad, a cooling fan, a water pump, and a sump, as illustrated in Fig. 2.

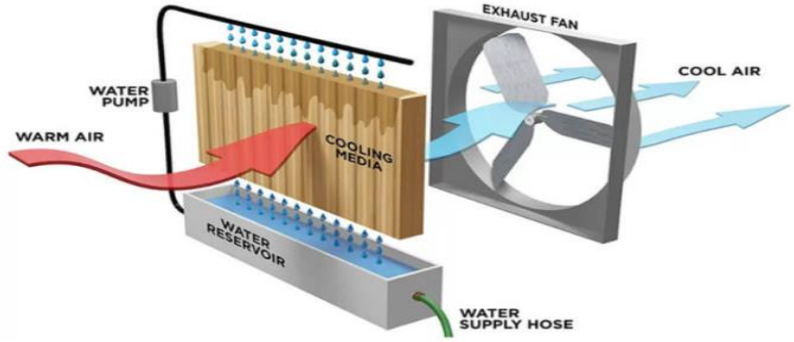

Fig. 2: Component of the fan pad Cooling System.

In the greenhouse, five cross-fluted cellulose pad panels were installed vertically on the wall opposite side of the exhaust fans, positioned on the north-facing side exposed to the prevailing wind. Each pad panel measured 10 cm in thickness, 60 cm in width, and 150 cm in height. On the leeward side, two exhaust fans were mounted to create negative pressure and facilitate air circulation inside the structure. The fans had power ratings of 250 W and 700 W, delivering airflow rates of 4,900 m^3/h and 9,990 m^3/h, respectively, with their operating speed regulated using an inverter. A 300 W automatic water pump supplied water to the pads through a distribution network. The distribution system consisted of a perforated polyvinyl chloride (PVC) pipe, 12.7 mm in diameter and 3 m in length, positioned directly above the cooling pads. Small holes, 3 mm in diameter, were drilled at 5 cm intervals along the pipe's upper surface, with the pipe end capped to maintain water pressure. A protective baffle was installed above the pipe to minimize unintended water leakage from the system.

The evaporative cooling system was scheduled to operate daily from 7 a.m. to 6 p.m. and was controlled through a mobile-based application. To enhance the cooling efficiency and reduce solar heat load inside the greenhouse, one of the structures was externally covered with a shading net that allowed 63% light transmission. The shading material had the following properties: a thickness of 3.5 mm, thermal conductivity of 0.037 $W \cdot m^{-1} \cdot K^{-1}$, thermal radiation transmittance below 0.001%, reflectance of 0.10, and emittance of 0.90.

Control system

An automated cooling control system was employed to continuously record data from multiple sensors, analyze the readings, and regulate the system's operation. In general, such an automatic control unit includes sensors for monitoring key process variables, actuators for system adjustment, a central controller, interface modules, a communication network, and proper power supplies. The measurement unit continuously collects data using 11 sensors, which are:

(a) Two Water temperature sensors.
(b) Seven Air temperature and Relative Humidity sensors.
(c) Two water flow rate sensors.

The Arduino Mega 2560 microcontroller, based on the ATmega 2560 chip, serves as the primary control component of the automation system. It sends and receives information from the sensors and devices connected to the data acquisition unit and the system correction unit. The mobile application was created on an

Android platform. It displays direct sensor values and enables the user to remotely control the actuators by using services from the cloud server.

Measurements and instrumentation

Shielded sensors for air temperature and relative humidity were utilized to monitor the greenhouse microclimate and ensure data reliability. The sensors were installed at a height of 1.5 m above ground level in four different positions: outside the cooling pad, immediately behind the pad, at a distance of 3 m from the pad, and near the exhaust fan.

Pad face air velocity

A digital fan anemometer was used to measure the average air speed on the pad surface. The anemometer can measure air speeds from 0.1 to 30 ms^{-1} with an accuracy of ±5%. For each greenhouse, the average air velocity on the pad surface was measured. Then, the average of all the measured points was calculated.

Evaporative cooling efficiency

The performance of an evaporative cooling system is mainly influenced by the reduction in air temperature, the wet-bulb depression, the rate of heat exchange between air and water, and the amount of water utilized during evaporation. The cooling efficiency (η, %) is determined as the ratio of the achieved cooling effect to the wet-bulb depression, as expressed in the following equation (ASHRAE, 2005):

$$\eta = \frac{t_o - t_{in}}{t_o - t_{wb}} \times 100 \qquad (1)$$

Where**:** **η** is the evaporative cooling efficiency (%)**,** $\mathbf{t_o}$ is the outdoor air temperature in (°c), $\mathbf{t_{in}}$ is the cooled air temprature behind the pads (°c), and $\mathbf{t_{wb}}$ is the wet-bulb air temperature of the outdoor (°c).

Cooling capacity

According to Sohani and Sayyaadi (2017) and Laknizi *et al.* (2019), the cooling capacity can be determined based on the temperature difference between the inlet and outlet air streams, as expressed in the following relation:

$$P_{air}\text{cooling} = m_{air}.c_p.(T_{out} - T_{in}) \qquad (2)$$

$$m_{air} = V.L.H.\rho \qquad (3)$$

Where**:** $\mathbf{m_{air}}$ is the mass flow rate of the supplied air ($kg \cdot s^{-1}$), **cp** denotes the specific heat capacity of air ($j \cdot kg^{-1} \cdot °c^{-1}$), **ρ** is the air density ($kg \cdot m^{-3}$), **v** represents the air velocity ($m \cdot s^{-1}$), **l** is the width of the cooling pad (m), and **h** is its height (m) .

RESULTS AND DISCUSSION

Indoor Air Temperature and Relative Humidity

In this experimental work, comparisons were made between indoor and outdoor air temperature and relative humidity during the period from 7:00 a.m. to 6:00 p.m. in August of each year (2022–2024). Fig. 3 illustrates the hourly variations of indoor temperature and humidity relative to outdoor conditions at different air velocities (1.0, 1.25, and 1.5 $m \cdot s^{-1}$) and a water flow rate of 2 $L \cdot min^{-1} \cdot m^{-2}$, both with and without the use of a shading net. The findings reveal a direct correlation between indoor and outdoor temperature: values rise gradually in the morning, reach maximum levels around noon, and then decline as solar radiation decreases later in the day. In contrast, the outdoor relative humidity was found to increase during nighttime hours and drop throughout the daytime in response to rising air temperature. The analysis further showed that the minimum daily average indoor temperature, 21.15 °C, together with an average relative humidity of 83.55%, was recorded at an air velocity of 1.25 $m \cdot s^{-1}$ when the shading screen was applied.

The recorded indoor air temperature varied between 17.90 and 24.42 °C, with relative humidity levels ranging from 64.12% to 90.23%. In comparison, the outdoor air temperature fluctuated between 25.91 and 41.25 °C, while outdoor relative humidity was within the range of 19.80–71.43%. The highest daily average indoor temperature, 23.88 °C, accompanied by an average relative humidity of 80.11%, occurred at an air velocity of 1.5 $m \cdot s^{-1}$ without the use of a shading screen.

In another observation, indoor air temperature was found to range from 19.24 to 27.92 °C with corresponding indoor humidity levels between 72.7% and 92.62%. During the same period, outdoor temperatures ranged from 27.93 to 41.25 °C, with relative humidity between 19.8% and 62.46%. It is important to note that the lowest recorded indoor temperature does not necessarily indicate optimal cooling performance, as variations in indoor and outdoor climatic conditions occurred due to the experiments being conducted on different days. Therefore, the most effective treatment can only be identified through the calculation of cooling efficiency for each case, which will be discussed in subsequent sections.

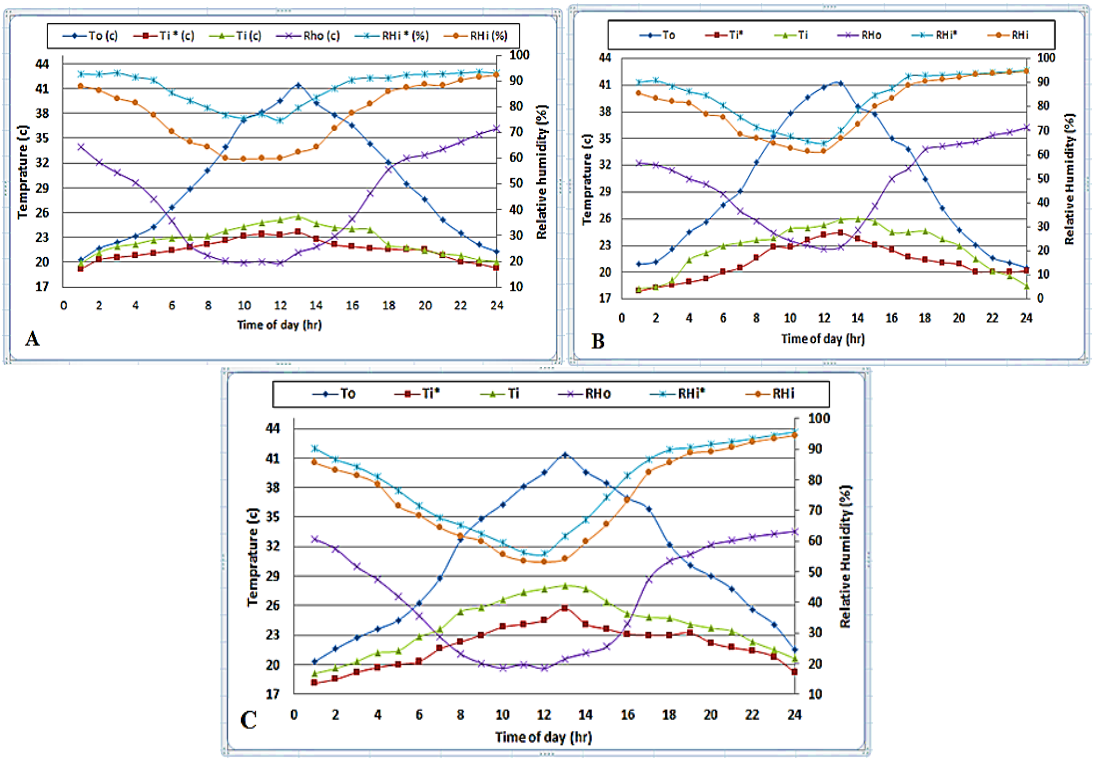

Fig. 3: Indoor air temperature and relative humidity compared with outdoor air temperature and relative humidity at different air velocities (A: 1 m s^{-1}, B: 1.25 m s^{-1}, C: 1.5 m s^{-1}) with a 2 L min^{-1} m^{-2} water flow rate.
(Note: * with shading net)

When the water flow rate was increased to 4 L·min^{-1}·m^{-2} under different air velocities (1.0, 1.25, and 1.5 m·s^{-1}), the results indicated that the lowest daily average indoor temperature, 20.48 °C, accompanied by a relative humidity of 77.02%, was obtained at an air velocity of 1.25 m·s^{-1} with the shading net applied. In this case, indoor temperatures ranged from 18.23 to 22.26 °C, while relative humidity varied between 62.33% and 86.62%. By comparison, the corresponding outdoor temperature fluctuated between 26.88 and 44.81 °C, with humidity levels ranging from 23.12% to 62.47%.

On the other hand, the highest daily average indoor temperature was 25.93 °C, along with an average relative humidity of 80.14%, which was recorded at an air velocity of 1.0 m·s^{-1} without shading. In this scenario, indoor air temperatures ranged between 19.72 and 28.43 °C, and relative humidity was within 69.43% to 89.64%. Meanwhile, outdoor conditions varied from 28.56 to 44.63 °C in temperature and 24.75% to 70.17% in relative humidity, as presented in Fig. 4.

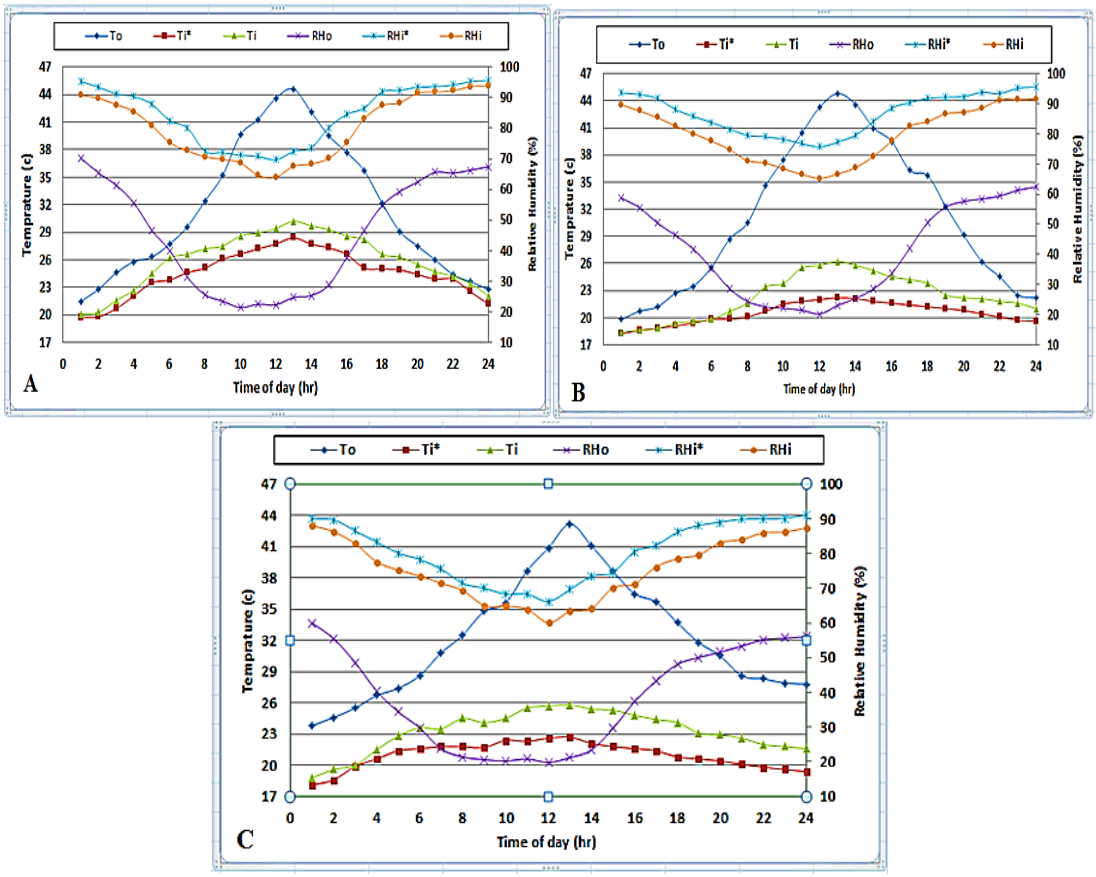

Fig. 4: Indoor air temperature and relative humidity compared with outdoor air temperature and relative humidity at different air velocities (A: 1 m s^{-1}, B: 1.25 m s^{-1}, C: 1.5 m s^{-1}) with 4 L min^{-1} m^{-2} of water flow rate.

At a higher water flow rate of 6 L·min^{-1}·m^{-2} combined with different air velocities (1.0, 1.25, and 1.5 m·s^{-1}), the results demonstrated that the minimum daily average indoor temperature was 23.32 °C, with a corresponding average relative humidity of 91.02%. This condition was achieved at an air velocity of 1.25 m·s^{-1} when the shading net was applied. Under these circumstances, indoor air temperature ranged from 18.6 to 25.70 °C, while relative humidity varied between 72.43% and 95.65%. The outdoor environment, in comparison, recorded temperatures from 28.86 to 40.82 °C and relative humidity between 24.74% and 78.16%.

Conversely, the highest daily average indoor temperature, 26.35 °C, accompanied by an average relative humidity of 80.14%, was observed at an air velocity of 1.5 m·s^{-1} without shading. In this case, indoor temperature fluctuated from 20.11 to 34.15 °C, and indoor humidity ranged from 67.64% to 93.84%. Meanwhile, the corresponding outdoor conditions showed temperature variations between 27.53 and 42.68 °C, with relative humidity ranging from 23.34% to 70.68%, as illustrated in Fig. 5.

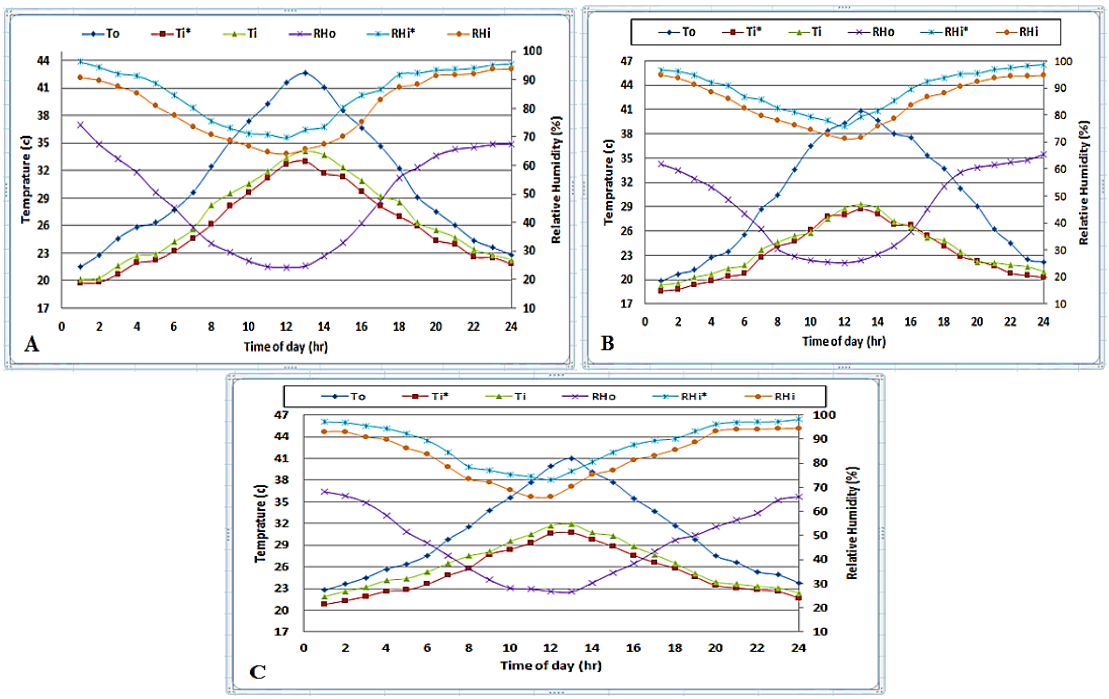

Fig. 5: Indoor air temperature and relative humidity compared with outdoor air temperature and relative humidity at different air velocities (A: 1 m s^{-1}, B: 1.25 m s^{-1}, C: 1.5 m s^{-1}) with 6 L min^{-1} m^{-2} of water flow rate.

Cooling effect

The cooling performance was evaluated daily from 7:00 a.m. to 6:00 p.m., and the results are summarized in Table 1 for different combinations of air velocities (1.0, 1.25, and 1.5 m·s^{-1}) and water flow rates (2, 4, and 6 L·min^{-1}·m^{-2}). The data showed that the cooling effect gradually increased throughout the morning, reaching its maximum around 1:00 p.m., after which it declined during the afternoon (2–6 pm.) .With the shading net, the maximum temperature difference between indoor and outdoor air, 22.6 °C, was achieved at an air velocity of 1.25 m·s^{-1} and a water flow rate of 4 L·min^{-1}·m^{-2}. Under these conditions, the temperature ranged from 1.6 °C to 22.6 °C. The lowest difference, 9.6 °C, occurred at 1.0 m·s^{-1} with a water flow rate of 6 L·min^{-1}·m^{-2}, with values ranging from 1.8 °C to 9.6 °C. In contrast, without the shading net, the maximum temperature difference recorded was 18.6 °C at 1.25 m·s^{-1} and 4 L·min^{-1}·m^{-2}, with a variation between 1.4 °C and 18.6 °C. The minimum difference, 8.5 °C, was observed at 1.0 m·s^{-1} with 6 L·min^{-1}·m^{-2}, ranging between 1.4 °C and 8.5 °C.

Table 1: The result of the test for the effect of different air velocities with different water flow rates on the cooling effect (°c).

	Air Velocity (ms^{-1})	Water flow rate ($L.min^{-1}.m^{-2}$)		
		2	**4**	**6**
Shading	**1**	17.8	16.2	9.6
	1.25	16.8	22.6	12.1
	1.5	15.6	20.5	10.3
Without shading	**1**	15.9	14.4	8.5
	1.25	15.3	18.6	11.5
	1.5	13.3	17.4	9.1

Cooling Efficiency

Figure 6 illustrates the influence of the shading net on cooling efficiency at various air velocities (1.0, 1.25, and 1.5 m·s^{-1}) under a water flow rate of 2 L·min^{-1}·m^{-2}. Without shading, the highest cooling efficiency was observed at 1.0 m·s^{-1}, where values ranged from 68.96% to 94.25%, with a daily average of 83.26%. The application of the shading net resulted in an efficiency enhancement, varying from 77.46% to 97.74%, with a mean of 88.27%, indicating an approximate increase of 5.01%.

At higher air velocities, the average cooling efficiency without shading declined to 80.88% at 1.25 m·s^{-1} and to 75.48% at 1.5 m·s^{-1}. With shading, the corresponding efficiencies were slightly higher, at 83.83% and 82.28%, respectively. This reduction in performance at higher air speeds can be attributed to insufficient pad saturation with water, which decreases evaporation efficiency since the air–water contact time becomes shorter. These findings are consistent with those reported by Franco *et al.* (2014).

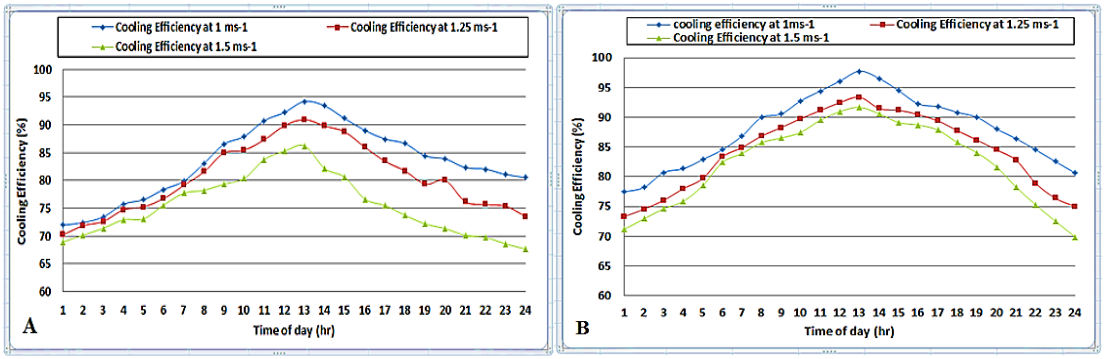

Fig. 6: The effect of shading net on cooling efficiency at different air velocities (1, 1.25, and 1.5 m s^{-1}) with 2 L min^{-1} m^{-2} of water flow rate. A: Without a shading net, B: with a shading net.

When the water flow rate was increased to 4 L·min^{-1}·m^{-2} under different air velocities (1.0, 1.25, and 1.5 m·s^{-1}), the best cooling performance was obtained at 1.25 m·s^{-1}, where efficiencies ranged from 76.08% to 97.63%, with a daily average of 88.71%. Incorporating a shading net further enhanced the performance, as it reduced solar radiation intensity and consequently lowered greenhouse air temperature. With shading, the cooling efficiency improved to a range of 86.95–99.16%, with an average daily efficiency of 94.35%, representing a 5.64% increase (Fig. 7) .

At the other air velocities, average daily cooling efficiency declined to 86.50% at 1.5 m·s^{-1} and 80.52% at 1.0 m·s^{-1}. With shading, these values increased to 91.33% and 83.82%, respectively. The observed trends can be explained by the effect of airflow rate on evaporation dynamics: as air velocity rises, the mass transfer coefficient and both latent and sensible heat exchange increase, leading to higher evaporation and improved efficiency. However, at 1.5 m·s^{-1}, the air–water contact time becomes too short, reducing the evaporation rate and lowering efficiency. These findings are consistent with those of Barzegar (2012).

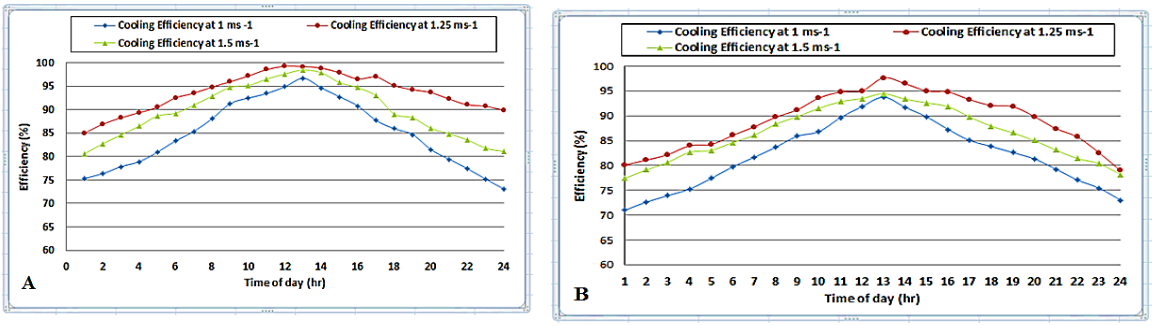

Fig. 7: The effect of shading net on cooling efficiency at different air velocities (1, 1.25, and 1.5 m s^{-1}) with 4 L min^{-1} m^{-2} water flow rate for A: with a shading net, B: without a shading net.

At a higher water application rate of 6 L·min⁻ ¹·m⁻ ² and under different airflow velocities (1.0, 1.25, and 1.5 m·s⁻ ¹), the maximum cooling efficiency was obtained at 1.25 m·s⁻ ¹, with values ranging between 61.35% and 81.27% and an average daily efficiency of 70.47%. When a shading net was applied, the performance improved slightly, reaching an average daily efficiency of 72.64% (an increase of 2.17%), with efficiency values between 54.79% and 85.87% (Fig. 8) .

At other air velocities, the daily average efficiency declined to 67.28% at 1.5 m·s⁻ ¹ and 65.30% at 1.0 m·s⁻ ¹, while the use of shading net resulted in slightly lower values of 64.24% and 62.78%, respectively. This behavior can be attributed to the influence of air velocity on evaporation dynamics: as velocity rises, both the mass transfer coefficient and the associated heat transfer increase, enhancing evaporation efficiency. However, at the highest velocity (1.5 m·s⁻ ¹), the limited contact time between air and water reduces the evaporation rate, which lowers the overall cooling performance. These findings are consistent with the observations of Barzegar *et al.* (2012) .

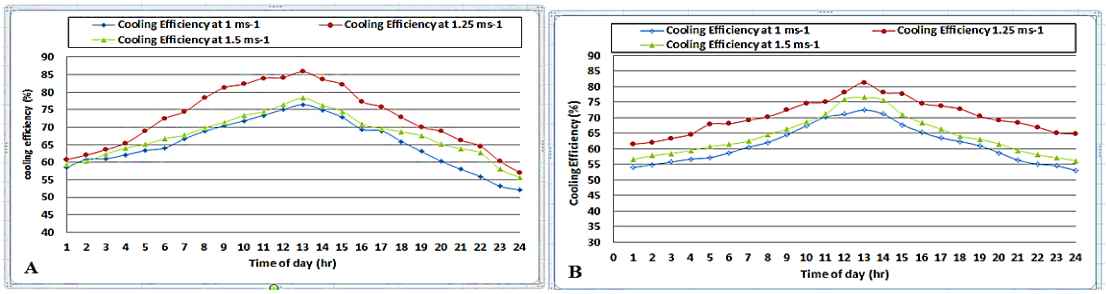

Fig. 8: The effect of shading net on cooling efficiency at different air velocities (1, 1.25, and 1.5 m s^{-1}) with 6 L min^{-1} m^{-2} water flow rate. A: with a shading net, B: without a shading net.

Cooling Capacity

Figure (9) illustrates the influence of a shading screen on the cooling capacity at different air velocities (1.0, 1.25, and 1.5 m·s⁻ ¹) under a water flow rate of 2 L·min⁻ ¹·m⁻ ². Without shading, the maximum cooling capacity was observed at 1.5 m·s⁻ ¹, ranging between 9.78 and 108.48 kW, with a daily average of 53.76 kW. When the shading net was applied, the cooling capacity improved, ranging between 69.77 and 127.24 kW, with an average daily value of 69.77 kW.

At lower air velocities, the average daily cooling capacity dropped to 47.21 kW at 1.25 m·s⁻ ¹ and 39.15 kW at 1.0 m·s⁻ ¹, whereas the use of shading increased these averages to 58.03 and 45.51 kW, respectively. This trend indicates that air velocity significantly affects the cooling

performance of direct evaporative systems, with the highest capacity consistently recorded at the highest airflow rate. These results align with the findings of Hassan *et al.* (2022).

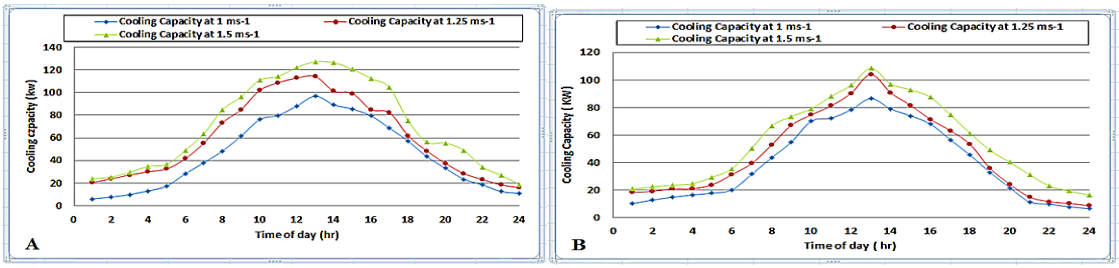

Fig. 9: The effect of shading net on cooling Capacity at different air velocities (1, 1.25, and 1.5 m s^{-1}) with a 2 L min^{-1} m^{-2} water flow rate. A: with a shading net, B: without a shading net.

When the water flow rate was raised to 4 L·min^{-1}·m^{-2}, the maximum cooling capacity was recorded at an air velocity of 1.5 m·s^{-1}. Under these conditions, the cooling capacity varied between 40.78 and 141.92 kW, with a daily average of 73.44 kW. The application of a shading net, which reduces heat accumulation and helps improve the greenhouse microclimate during hot summer periods, further enhanced the performance, raising the daily average to 91.96 kW and expanding the capacity range to 46.49–167.21 kW, as illustrated in Figure 10.

At lower air velocities, the daily average cooling capacity decreased to 59.44 kW at 1.25 m·s^{-1} and 30.17 kW at 1.0 m·s^{-1}. With shading, however, these averages increased to 72.07 and 38.01 kW, respectively.

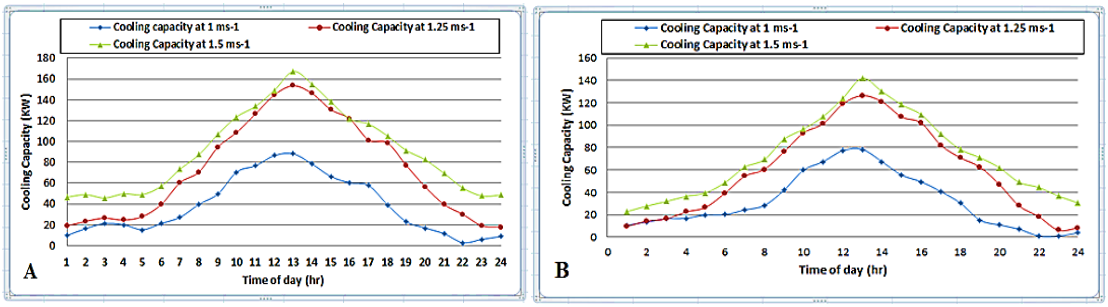

Fig. 10: The effect of shading net on cooling Capacity at different air velocities (1, 1.25, and 1.5 m s^{-1}) with 4 L min^{-1} m^{-2} water flow rate. A: with a shading net, B: without a shading net.

At a water flow rate of 6 L·min^{-1}·m^{-2}, the maximum cooling capacity was obtained at an air velocity of 1.5 m·s^{-1}, where values ranged from 11.71 to 78.16 kW, with a daily average of 41.97 kW. The addition of a shading net further enhanced the system performance, increasing the daily average capacity to 45.73 kW and widening the range to 18.15–86.24 kW, as shown in Figure 11.

At lower air velocities, the daily average cooling capacity declined to 34.97 kW at 1.25 m·s^{-1} and 22.34 kW at 1.0 m·s^{-1}. However, when shading was applied, the averages increased to 43.63 and 27.57 kW, respectively.

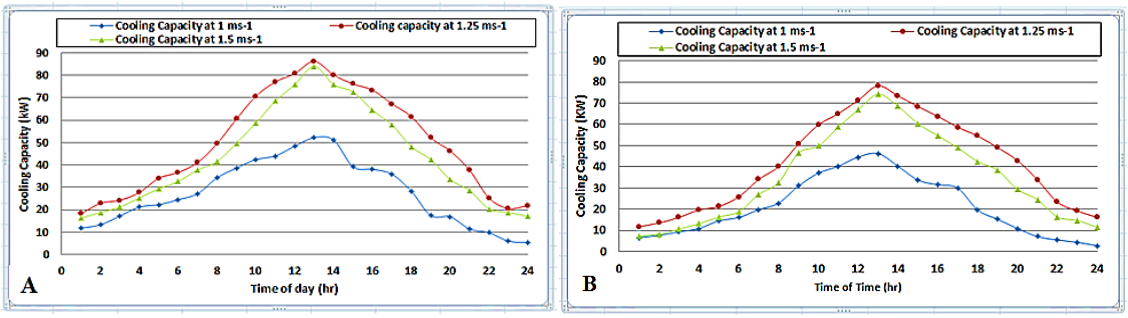

Fig. 11: The effect of shading net on cooling Capacity at different air velocities (1, 1.25, and 1.5 m s^{-1}) with 4 L min^{-1} m^{-2} water flow rate. A: with a shading net, B: without a shading net.

Conclusion

Both air velocity and water flow rate significantly influenced the temperature reduction inside the greenhouse. The maximum temperature drop (22.6 °C) was achieved at a water flow rate of 4 $L \cdot min^{-1} \cdot m^{-2}$ and an air velocity of 1.25 $m \cdot s^{-1}$ under shaded conditions.

The interaction between air velocity and water flow rate significantly influenced cooling efficiency. The peak efficiency (94.36%) was observed at an air velocity of 1.25 $m \cdot s^{-1}$ and a water flow rate of 4 $L \cdot min^{-1} \cdot m^{-2}$ with the application of shade nets.

Cooling capacity increased with air velocity. The maximum value (91.96 kW) was observed at 1.5 $m \cdot s^{-1}$ with a water flow rate of 4 $L \cdot min^{-1} \cdot m^{-2}$ under shading.

The findings highlight the advantage of using shading nets in conjunction with evaporative cooling systems, as they reduce solar radiation intensity, stabilize the microclimate, and contribute to a lower air temperature within the greenhouse.

REFERENCES

Ahmed, H.A.; Al-Faraj, A.A. and Abdel-Ghany, A.M. (2016). Shading greenhouses to improve the microclimate, energy and water saving in hot regions: A review. Sci. Hort. 201: 36–45.

Ali Sohani, Hoseyn Sayyaadi., (2017). Design and retrofit optimization of the cellulose evaporative cooling pad systems at diverse climatic conditions, Applied Thermal Engineering 123: 1396–1418, http://dx.doi.org/10.1016/j.applthermaleng.20 17.05.120

ASHRAE., (2005). "Handbook of fundamentals" American Society of Heating, Refrigerating, and Air Conditioning Engineers, Atlanta, GA 30329.

Barzegar, M.; Layeghi, M.; Ebrahimi, G.; Hamzeh, Y. and Khorasani, M. (2012). Experimental evaluation of the performances of cellulosic pads made out of Kraft and NSSC corrugated papers as evaporative media. Energy Conversion and Management, 54(1): 24-29.

Dağtekin, M.; Karaca, C.; Yıldız, Y.; Başçetinçelik, A. and Paydak, Ö. (2011). The effects of air velocity on the performance of pad evaporative cooling systems. Afr. J. Agric. Res. 6: 1813-22.

Franco, A.; Valera, D.L.; Madneno, A. and Pena A. (2010). Influence of water and air-flow on the performance of cellulose evaporative cooling pads used in Mediterranean greenhouses. T. ASABE. 52: 565-76.

Franco, A.; Valera, D. L. and Peña, A. (2014). Energy efficiency in greenhouse evaporative cooling techniques: Cooling boxes versus cellulose pads. Energies, 7(3): 1427-1447.

Graamans, L.; Baeza, E.; Dobbelstena, A.; Tsafaras, I. and Stanghellini, C. (2018). Plant factories versus greenhouses: Comparison of resource use efficiency. Agric. Syst., 160: 31–43.

Hassan, Z.; Misaran, M.S.; Siambun, N.J. and Adzrie, M. (2022). The effect of air velocity on the performance of the direct evaporative cooling system. IOP Conf. series: Materials

science and Engineering, Sci. Eng. 1217012016.2022.

Jin Ryu, M.; Ki Ryu, D.; Ok Chung, S.; Kun Hur, Y.; Oh Hur, S.; Jung Hong, S.; Hoon Sung, J. and Hun Kim, H. (2014). Spatial, vertical, and temporal variability of ambient environments in strawberry and tomato greenhouses in winter. Journal of Biosystems Engineering, 39(1): 47–56.

Karaca, C., Dağtekin, M., Y. Yildiz, A. Başçetinçelik and Ö. Paydak (2011). The effects of air velocity on the performance of pad evaporative cooling systems. African Journal of Agricultural Research, 6(7), 1813-1822.

Laknizi, A.; Mahdaoui, M.; Ben Abdellah, A.; Anoune, K.; Bakhouya, M. and Ezbakhe, H. (2019). Performance analysis and optimal parameters of a direct evaporative pad cooling system under the climate conditions of Morocco. Case Studies in Thermal Engineering, 13. https://doi.org/10.1016/j.csite.2018.11.013.

Lee SH, Lee W.L. (2013). Site verification and modeling of desiccant-based system as an alternative to conventional air conditioning systems for wet markets. Energy; 55: 1076–83.

Xu, J.; Li, Y.; Wang, R.Z.; Liu, W. and Zhou, P. (2015). Experimental performance of evaporative cooling pad systems in greenhouses in humid subtropical climates. Appl. Energy 2015, 138: 291–301.

تأثير معدل تدفق المياه وسرعة الهواء على أداء نظام التبريد التبخيري في الصوب الزراعية

أحمد عبدالحميد شكر، أيمن حافظ عيسى، إيهاب الصعيدي، أحمد توفيق طه

قسم الهندسة الزراعية والنظم الحيوية – كلية الزراعة – جامعة المنوفية

الملخص العربي

لقد أصبح تغير المناخ أحد أهم العوامل المؤثرة في الإنتاج الزراعي. يمكن استخدام التحكم البيئي داخل الصوب الزراعية لتجنب تأثير التغيرات البيئية المختلفة. الهدف الرئيسي من هذا العمل هو تحسين المعاملات التشغيلية لاستخدام نظام التبريد التبخيري مثل تدفق المياه وسرعة الهواء. لتحقيق ذلك، أجريت التجارب عند ثلاث معدلات مختلفة لتدفق المياه (٢ و٤ و٦ لتر. دقيقة$^{-1}$ م$^{-2}$) وثلاث سرعات هواء مختلفة (١,٠ و١,٢٥ و١,٥ م ثانية$^{-1}$) على درجة حرارة الهواء والرطوبة النسبية وكفاءة التبريد وسعة التبريد في الصوبة الزراعية. أظهرت النتائج وجود علاقة بين درجة حرارة الهواء الداخلي والخارجي حيث ترتفع درجة الحرارة في الصباح الباكر من اليوم وتصل إلى ذروتها عند الظهر ثم تبدأ في الانخفاض مع زيادة الإشعاع الشمسي وانخفاضه. تزداد الرطوبة النسبية للهواء الخارجي أثناء الليل وتنخفض أثناء النهار مع زيادة درجة حرارة الهواء. سُجِّلت أعلى قيمة لكفاءة التبريد (٩٤,٣٦%) عند سرعة هواء ١,٢٥ م/ثانية$^{-1}$ ومعدل تدفق ماء ٤ لتر دقيقة $^{-1}$ م $^{-2}$ فوق الوسادة عند استخدام شبكات التظليل، بينما سُجِّلت أعلى قيمة لقدرة التبريد عند (٩١,٩٦ كيلو واط) عند سرعة هواء ١,٥ م/ثانية$^{-1}$ ومعدل تدفق ماء ٤ لتر دقيقة $^{-1}$ م $^{-2}$. وتوصي النتائج إلى أن المتغيرات الأكثر فعالية كانت عند سرعة هواء ١,٢٥ م/ثانية$^{-1}$ مع معدل تدفق مياه ٤ لتر دقيقة $^{-1}$ م $^{-2}$ مع استخدام شبكة التظليل.

الكلمات المفتاحية: التبريد التبخيري، الرطوبة النسبية، كفاءة التبريد، سعة التبريد.